Development 137, 93-102 (2010) doi:10.1242/dev.041459

C. elegans STRADα and SAD cooperatively regulate neuronal polarity and synaptic organization

Joanne S. M. Kim[1,2], Wesley Hung[2], Patrick Narbonne[3], Richard Roy[3] and Mei Zhen[1,2,*]

SUMMARY

Neurons are polarized cells with morphologically and functionally distinct axons and dendrites. The SAD kinases are crucial for establishing the axon-dendrite identity across species. Previous studies suggest that a tumour suppressor kinase, LKB1, in the presence of a pseudokinase, STRADα, initiates axonal differentiation and growth through activating the SAD kinases in vertebrate neurons. STRADα was implicated in the localization, stabilization and activation of LKB1 in various cell culture studies. Its in vivo functions, however, have not been examined. In our present study, we analyzed the neuronal phenotypes of the first loss-of-function mutants for STRADα and examined their genetic interactions with LKB1 and SAD in *C. elegans*. Unexpectedly, only the *C. elegans* STRADα, STRD-1, functions exclusively through the SAD kinase, SAD-1, to regulate neuronal polarity and synaptic organization. Moreover, STRD-1 tightly associates with SAD-1 to coordinate its synaptic localizations. By contrast, the *C. elegans* LKB1, PAR-4, also functions in an additional genetic pathway independently of SAD-1 and STRD-1 to regulate neuronal polarity. We propose that STRD-1 establishes neuronal polarity and organizes synaptic proteins in a complex with the SAD-1 kinase. Our findings suggest that instead of a single, linear genetic pathway, STRADα and LKB1 regulate neuronal development through multiple effectors that are shared in some cellular contexts but distinct in others.

KEY WORDS: *C. elegans*, LKB1, SAD kinases, STRAD, Neuronal polarity

INTRODUCTION

Neurons are polarized cells that receive inputs at dendrites and transmit electrical signals along axons. They undergo a series of morphological transformations to establish axonal and dendritic identities (Dotti et al., 1988). In cultures, a nascent neuron, or a neuron undergoing re-polarization, initially extends multiple neurite projections. The fastest growing neurite develops into an axon and the rest become dendrites. As the axon elongates and contacts its targets, synapses are established to allow for communication in neuronal networks. Recent studies have begun to reveal regulators for axon/dendrite polarization. These include both extrinsic cues, such as morphogens and growth factors, and intrinsic mechanisms, including signalling kinase cascades, their associated scaffolding proteins and factors affecting actin cytoskeleton and microtubule dynamics (reviewed in Arimura and Kaibuchi, 2005; Barnes and Polleux, 2009; Conde and Caceres, 2009; Wiggin et al., 2005).

Although many proposed polarity regulators were characterized in dissociated neuronal cultures, only few have been verified to play a role in the axon/dendrite specification in vivo. One such example is a family of Ser/Thr kinases called SAD (synapses of amphids defective). Initially isolated from a *C. elegans* screen for mutations affecting synapse development, SAD-1 was the first known regulator for both neuronal polarity and synaptic organization in vivo (Crump et al., 2001; Hung et al., 2007). In *sad-1* loss-of-function mutants, both pre-synaptic vesicle and active zone proteins fail to be restricted to the axons of motor and sensory neurons. Synaptic vesicles also fail to form tight clusters in *sad-1* mutants, implying aberrant synaptic organization in addition to defects in neuronal polarity (Crump et al., 2001; Hung et al., 2007). SAD-1 kinase activity is crucial during the establishment, but largely dispensable for the maintenance, of neuronal polarity and synaptic organization (Kim et al., 2008).

The SAD kinases display functional conservation in neuronal polarity across species. Two mouse homologs of SAD-1, SAD-A and SAD-B, function redundantly to establish the axon/dendrite polarity in hippocampal and cortical neurons (Kishi et al., 2005). Cortical neurons of the *SAD-A*$^{-/-}$;*SAD-B*$^{-/-}$ (*Brsk2*$^{-/-}$;*Brsk1*$^{-/-}$ – Mouse Genome Informatics) double knock-out mice show aberrant migration and neurite differentiation, and cultured hippocampal neurons project neurites with no distinct axonal or dendritic properties (Kishi et al., 2005). Reducing the expression of rat SAD-B in the mature central nervous system was also shown to affect neurotransmitter release (Inoue et al., 2006).

The SAD kinases are distantly related to the AMPK kinases (Lizcano et al., 2004). LKB1, a tumour suppressor protein and a master Ser/Thr kinase for an AMPK subfamily of kinases, can phosphorylate the mammalian SAD kinases in vitro (Lizcano et al., 2004). LKB1 was also required for neuronal polarization in vivo (Barnes et al., 2007; Shelly et al., 2007). Similar to the defects observed in the *SAD-A*$^{-/-}$;*SAD-B*$^{-/-}$ double knock-out mice, cortical neurons of mice lacking LKB1 failed to differentiate distinct axons and dendrites, and the level of phosphorylation in the activating T-loop of SAD kinases in these neurons was drastically decreased (Barnes et al., 2007). Ectopic co-expression of SAD-A and LKB1 in non-neuronal cells resulted in robust phosphorylation of both SAD-A and its sole known substrate, Tau (Kishi et al., 2005), supporting that LKB1 is a direct activator of the SAD kinases in vivo (Barnes et al., 2007).

[1]Department of Molecular Genetics, University of Toronto, Toronto, Ontario, M5S 1A8, Canada. [2]Samuel Lunenfeld Research Institute, Mount Sinai Hospital, Toronto, Ontario, M5G 1X5, Canada. [3]Department of Biology, McGill University, Montreal, Quebec, H3A 1B1, Canada.

*Author for correspondence (zhen@lunenfeld.ca)

Accepted 26 October 2009

LKB1 is the mammalian homolog of *par-4*, one of the six *par* (*partitioning defective*) genes that control cell polarity in *C. elegans* embryos (Kemphues et al., 1988; Watts et al., 2000). LKB1/PAR-4 has since been established as a general regulator for epithelial cell polarity and cell growth in both invertebrates and vertebrates (Baas et al., 2004; Martin and St Johnston, 2003; Watts et al., 2000). Association of LKB1 with two co-factors, STRAD (Baas et al., 2003) and MO25 (Boudeau et al., 2003; Boudeau et al., 2004; Milburn et al., 2004), was implicated for the stability (Baas et al., 2003; Boudeau et al., 2003), optimal activity (Baas et al., 2004; Lizcano et al., 2004) and nuclear-to-cytoplasmic translocation (Baas et al., 2003; Boudeau et al., 2003; Dorfman and Macara, 2008) of LKB1 in various cell culture studies.

STRAD is a STE-20-related pseudokinase missing some of the essential residues for kinase activity (Baas et al., 2003). The alpha (α) version of STRAD (STRADα) was more effective in enhancing the LKB1 activity in vitro than the beta form of STRAD (Lizcano et al., 2004). Recent studies also implied the importance of STRADα in LKB1-mediated neuronal polarization (Barnes et al., 2007; Shelly et al., 2007). The siRNA-mediated knock-down of STRADα in cultured rat hippocampal neurons abolished the axon-dendrite distinction, similar to knocking down LKB1 (Shelly et al., 2007). Co-transfection of STRADα was also required for the excessive axon formation induced by LKB1 over-expression in cultured mouse neurons (Barnes et al., 2007). However, STRADα was dispensable for LKB1-induced supernumerary axon differentiation in rat hippocampal cultures (Shelly et al., 2007). The effects of STRADα manipulation in vitro could be cell-context dependent, and the analysis of STRADα loss-of-function mutants is important to establish the physiological functions of STRADα.

To investigate the physiological functions of STRADα and its interplay with LKB1 and SAD in vivo, we examined the neuronal phenotypes of the loss-of-function mutants for the sole *C. elegans* STRADα and LKB1 homologs, *strd-1* and *par-4*, respectively. We also determined their genetic interactions with *sad-1*. Although both PAR-4 and STRD-1 affect neuronal polarity, surprisingly only STRD-1 shares a linear genetic pathway with SAD-1 to regulate neuronal polarity and synaptic organization. STRD-1 also associates with SAD-1 and modulates its sub-cellular localization. PAR-4, by contrast, also functions through additional effectors to regulate neuronal polarity. These findings suggest that STRD-1 and SAD-1 form a complex that is crucial for neuronal development in *C. elegans*, whereas PAR-4 and STRD-1 can have distinct effectors to regulate neuronal polarity.

MATERIALS AND METHODS

Strains

All strains were cultured on NGM plates (Brenner, 1974) seeded with OP50. N2 was used as the wild-type strain. The *sad-1(ky289)*-null allele (Crump et al., 2001; Hung et al., 2007) was used for all *sad-1* analyses. Two *strd-1* alleles were used: *rr91*, identified in a screen for a hyperplasia germline phenotype in dauers, is maintained in a *daf-2*(*e1370*) background (P.N. and R.R., unpublished); *ok2283* is a deletion- and protein-null allele four times out-crossed against N2. *daf-2*(*e1370*) had no effect on the neuronal phenotypes (data not shown). For all *par-1* and most *par-4* analyses, the temperature-sensitive (*ts*) alleles *zu310ts* (K. Kemphues, Cornell University, NY, USA) and *it57ts* (Morton et al., 1992) were used, respectively. For phenotypic analyses, L4-stage *zu310ts*, *it57ts* and control strains were cultured at 15°C and transferred to 22°C when they carried embryos (primarily at 4- to 16-cell stages). Their progenies were examined 24 hours post-L4. For the temperature-shift experiments, *it57ts* embryos were cultured at 15°C until the desired larval stages were reached before being shifted to 22°C; their phenotypes were examined 24 hours post-L4. Non-conditional alleles of *par-4*, *it33* and *it75* (Morton et al., 1992; K. Kemphues) are marked by *dpy-21(e428)* and maintained as heterozygous animals. Homozygous Dpy animals that laid dead eggs were examined for their polarity phenotypes. *nab-1*(*ok943*), *rpm-1*(*ju44*) and *dsh-2(or302)* were used for analyses. Only *strd-1* and *par-4* allele information was given in figures for simplicity.

pJH21 [P_{unc-25}-*sad-1*::*gfp* (L,S)], pJH731 [P_{unc-25}-*gfp*::*sad-1*(L)] or pJH1090 [P_{unc-25}-*rfp*::*sad-1*(S)] were co-injected with a P_{lin-15}-*lin-15* into *lin-15* (*n765ts*) animals and integrated into the *C. elegans* genome to generate *hpIs1*, *hpIs99* and *hpIs105*, respectively. *juIs1*, *oxIs22* and *kyIs105* have been previously described (Dwyer et al., 2001; Zhen et al., 2000; Zhen and Jin, 1999). The *strd-1* transcriptional reporter, pJH1258 (P_{strd-1}-*nls*::*gfp*), was co-injected with a P_{lin-15}-*lin-15* into *lin-15*(*n765ts*). For rescue experiments, pJH73 ($P_{unc-115}$-*sad-1*), pJH1139 (P_{unc-25}-*par-4*), pJH1215 (P_{unc-25}-*strd-1*) or pJH1369 [P_{unc-25}-*strd-1*(D175A)] was co-injected with a P_{odr-1}-*gfp* into the indicated strains. For sub-cellular localization experiments, pJH1735 (P_{unc-25}-*rfp*::*strd-1*) was injected into *hpIs1* and *hpIs99* animals and pJH1673 (P_{unc-25}-*gfp*::*strd-1*) was injected into *hpIs105* animals. For punctum counting, pJH1090 [P_{unc-25}-*rfp*::*sad-1*(S)] was injected to N2 animals, and the same chromosomal array crossed into *strd-1* mutants. For bi-fluorescent reconstitution experiments, pJH1755 (P_{unc-25}-*nyfp*::*strd-1*) and pJH1756 [P_{unc-25}-*cyfp*::*sad-1*(L)] were co-injected or sequentially injected into N2. Co-injection and sequential injection of pJH1755 with P_{unc-25}-*cyfp*, and of pJH1756 with P_{unc-25}-*nyfp*, served as controls.

Plasmids

pJH1139 (P_{unc-25}-*par-4*) was generated by inserting the 1.8 kb *par-4* cDNA (Labbé, McGill University, QC, Canada) into pJH540 (P_{unc-25}). pJH1215 (P_{unc-25}-*strd-1*) and pJH1673 (P_{unc-25}-*gfp*::*strd-1*) were generated by inserting the 3.5 kb *strd-1* genomic coding region into pJH540 or pJH401 (P_{unc-25}::*gfp*), respectively. pJH1735 (P_{unc-25}-*rfp*::*strd-1*) was generated by inserting *wCherry* (*mCherry* optimized for expression in *C. elegans*; A. Desai, University of California, San Diego, CA, USA) and genomic *strd-1* into pJH540, respectively. pJH1258 (P_{strd-1}::*gfp*) was generated by inserting the 5.2 kb upstream region of the operon CEOP3708 into pPD95.67 (Fire et al., 1990). pJH21 and pJH73 were previously described (Hung et al., 2007). pJH731 and pJH1090 were generated by inserting long- and short-isoform encoding sequences of *sad-1* under the *unc-25* promoter with *gfp* and *mCherry*, respectively. pJH1369 was generated by mutating the genomic sequence (D175 to A) of pJH1215, and cloning a sequencing-verified mutated region back into pJH1215. pJH1755 and pJH1765 were generated by adding the *nyfp* and *cyfp* fragments (Z. W. Wang, University of Connecticut, CT, USA) to the 5′ end of *strd-1* in pJH1215, or of *sad-1* long isoform in pJH730, which is identical to pJH731 but without *gfp*.

Fluorescent marker analyses and immunostaining

To analyze *juIs1* and *oxIs22* in L1 animals, early L1s were hatched from eggs harvested from hypochlorite-treated gravid adults and were fixed as previously described (Kim et al., 2008). To visualize ventral cord (VD) puncta in adults, double-stranded *unc-30* RNA was synthesized from pJH573 and injected to *juIs1* adults as described previously (Hallam et al., 2002; Hung et al., 2007). The selective elimination of *juIs1* expression in dorsal cord (DD) neurons was confirmed by the lack of GFP signals in DD cell bodies, and their progenies were scored 24 hours post-L4. Wholemount staining was performed as described using anti-SAD-1 (Hung et al., 2007).

Biochemistry

C. elegans lysate preparation, immunoprecipitation (IP) and immunoblotting (IB) were performed as described previously (Liao et al., 2004). For IP, mouse monoclonal anti-GFP (Roche) and anti-mouse IgG (Santa Cruz Biotechnology) were used. For IB, a rabbit polyclonal antibody against heat-denatured GFP (Nakamura et al., 2008), monoclonal mouse anti-β-tubulin E7 (Developmental Studies Hybridoma Bank) and α-STRD-1, a rabbit antibody against amino acid 1-332, were used.

For the kinase assay, 200 μg of lysates were pre-cleared with mouse IgG and Protein A agarose beads (Roche) and incubated with mouse anti-GFP (Roche) and Protein A beads at 4°C overnight. Washed beads were resuspended in 13 μL of kinase buffer (Kim et al., 2008), to which 1 μg of

recombinant human TAU (Sigma) and 1 μL of 1 mM ATP were added, and incubated at 22°C for 30 minutes. 10 μL supernatant was subjected to IB with anti-TAU pS262 (Invitrogen).

Statistics

Significance testing employed the Wilcoxon rank-sum test (VD phenotypes), the Proportion test (DD and ASI phenotypes) and *t*-test [SAD-1 punctum counts in R(v2.6.2)]. Analysis with Punctaanalyser was previously described (Kim et al., 2008).

RESULTS

Loss-of-function mutations in STRADα/STRD-1 and LKB1/PAR-4 lead to neuronal polarity defects in *C. elegans*

STRD-1 and PAR-4 are the sole *C. elegans* homologs of the mammalian STRADα and LKB1, respectively. To determine whether they are required for the development of the nervous system, we examined neuronal polarity and synaptic phenotypes in the respective loss-of-function mutants.

Two loss-of-function alleles for *strd-1* were employed for analyses. *strd-1*(*rr91*) was identified in a genetic screen for mutants with germline hyperplasia (P.N. and R.R., unpublished) and harbours a mutation that leads to a premature stop codon at Q322 (see Fig. S1 in the supplementary material). *strd-1*(*ok2283*) deletes from amino acid R174 onward and is a protein-null allele (Fig. 4D; also see Fig. S1 in the supplementary material). In our analyses below, both alleles of *strd-1* displayed similar phenotypes, slightly stiff but active locomotion (see Movies in the supplementary material) and reduced brood sizes (data not shown), but had otherwise superficially normal larval development.

A complete loss of function in PAR-4 disrupts the asymmetric partitioning of developmental determinants during the first two embryonic cell divisions and leads to subsequent embryonic lethality (Kemphues et al., 1988; Morton et al., 1992). We therefore employed the strongest temperature-sensitive (*ts*) allele of *par-4*, *it57ts*, that harbours a mutation in the kinase domain and exhibits 100% embryonic lethality at non-permissive temperatures (Kemphues et al., 1988; Morton et al., 1992; Watts et al., 2000). *it57ts* embryos were cultured at a permissive temperature but shifted during the first few cell divisions to a non-permissive temperature for phenotypic observations. We also examined two non-conditional alleles of *par-4*, *it33* and *it75*, where some homozygous progenies from the *par-4(+/–)* heterozygous parents survive embryogenesis owing to maternal contribution of PAR-4 (Kemphues et al., 1988; Morton et al., 1992).

We first examined neuronal polarity in GABAergic motoneurons (Hallam et al., 2002; Hung et al., 2007; Kim et al., 2008). Axons of the six embryonically-born GABAergic DD neurons innervate ventral body wall muscles in the first larval stage (L1) animals (Fig. 1A, top illustration). In wild-type animals, the pre-synaptic *juIs1* marker, which expresses a GFP-tagged synaptic vesicle protein in GABAergic neurons (P_{unc-25}-*snb-1*::*gfp*) (Zhen and Jin, 1999), and the post-synaptic *oxIs22* marker, a GFP-tagged GABA-A receptor (P_{unc-49}-*unc-49*::*gfp*) (Zhen et al., 2000), appear exclusively along the ventral nerve cord (Fig. 1A,B). By contrast, 100% of *sad-1*(*ky289*)-null mutants display numerous ectopic fluorescent signals along the dorsal nerve cord (Fig. 1A,B), representing a fully penetrant polarity defect as previously reported (Crump et al., 2001; Hung et al., 2007). Both *par-4*(*it57ts*) and *strd-1*(*rr91*) mutants showed polarity defects in L1 DD neurons (Fig. 1A,B). It is noteworthy, however, that although *strd-1* mutants displayed a polarity defect as severe as *sad-1* mutants, both the expressivity and penetrance of the polarity defect were considerably lower in *par-4* mutants (Fig. 1A,B). The phenotypic severity in each mutant was also consistent between the pre-synaptic and post-synaptic markers (Fig. 1A,B), suggesting that the ectopic puncta, probably representing synapses, imply a failure in restricting axonal identity to the ventral neurites.

We further examined neuronal polarity in ventral cord (VD) neurons, the post-embryonically derived GABAergic motoneurons, in adults. As there is no VD neuron-specific marker, we performed *unc-30* RNAi on *juIs1* animals to selectively eliminate the expression of SNB-1::GFP in dorsal cord (DD) neurons (Hallam et al., 2002; Hung et al., 2007; Materials and methods). In wild-type adults, VD axons innervate ventral body wall muscles (Fig. 1C, top illustration). This is faithfully reflected by the localization of the majority of VD-derived pre-synaptic SNB-1::GFP puncta along the ventral, but not the dorsal, nerve cord in adults (Fig. 1C,D). By contrast, *sad-1*-null mutants fail to restrict the pre-synaptic marker to VD axons and display ectopic puncta along the dorsal cord (Fig. 1C,D).

Both *par-4*(*it57ts*) and *strd-1*(*rr91*) mutants also displayed VD polarity defects (Fig. 1C-D). Consistent with the observations made from the L1 DD neurons, although the severity of the VD polarity defect in *strd-1* adults was similar to that in *sad-1*-null animals, *par-4* mutants (both *ts* and non-conditional alleles) displayed a considerably weaker phenotype (Fig. 1C,D; also see Fig. S2A in the supplementary material). The VD defects in both *par-4* and *strd-1* mutants were fully rescued when PAR-4 or STRD-1 were expressed under a GABAergic neuron-specific *unc-25* promoter (Fig. 3B; also see Fig. S4A in the supplementary material), consistent with them functioning cell-autonomously to regulate polarity.

Finally, failure to restrict the pre-synaptic marker to axons was consistently observed in the ASI sensory neurons of *par-4*(*it57ts*) and *strd-1*(*ok2283*) mutants with an identical trend in their phenotypic severity (see Fig. S3A,B in the supplementary material). Therefore, both *par-4* and *strd-1*, like *sad-1*, regulate the polarity of multiple *C. elegans* neurons.

Mutations in *strd-1* cause synaptic organization defects

In addition to neuronal polarity, SAD-1 kinase also regulates synaptic organization (Crump et al., 2001; Hung et al., 2007). In wild-type adults, round and discrete *juIs1* puncta, representing SNB-1::GFP pre-synaptic vesicle clusters, are observed in the DD axons along the dorsal nerve cord (Fig. 1Ei,iii, left illustration). In *sad-1*-null mutants, the SNB-1::GFP puncta appear diffuse or smaller (Fig. 1Eiv, right illustration) as previously reported (Crump et al., 2001). *strd-1*(*ok2283*) mutants showed diffuse and smaller puncta qualitatively identical to *sad-1*-null mutants (Fig. 1Eiii-v). This is reflected by the wider distribution curve of the punctum widths in *strd-1* mutants when compared with that of wild-type animals, but is similar to the distribution pattern in *sad-1* mutants (Fig. 1E, bottom density graph). Therefore, like SAD-1, STRD-1 is also required for both neuronal polarity and synaptic organization. By contrast, all alleles of *par-4* animals showed normal SNB-1::GFP punctum morphology (Fig. 1Ei-ii, data not shown), and there was no difference in the distribution of the punctum widths between *par-4*(*it57ts*) and wild-type animals (Fig. 1E, top density graph).

strd-1 and *sad-1* regulate neuronal polarity in a genetic pathway parallel to *par-4* and *par-1*

Our analyses consistently showed that although *strd-1* mutants phenocopied *sad-1* mutants, *par-4* mutants displayed weaker defects than those of *strd-1* or *sad-1* mutants. These milder phenotypes could be due to allelic effects: the loss of function in *it57ts* at non-

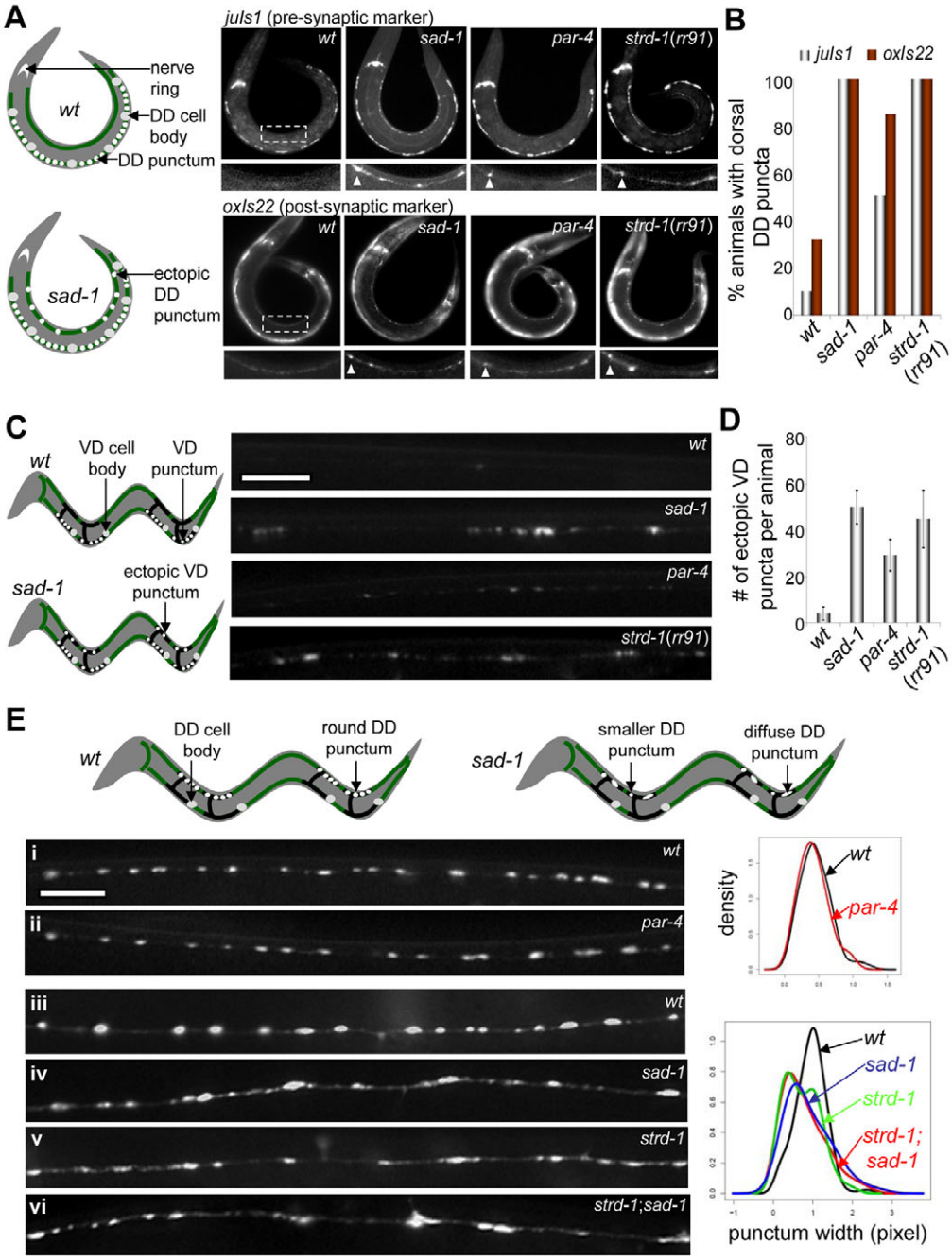

Fig. 1. Loss-of-function mutations in *strd-1* and *par-4* lead to neuronal defects. (**A**) Polarity defects in dorsal cord (DD) neurons in L1 larvae. In wild-type (*wt*) animals, the pre-synaptic *juls1* marker in DDs and post-synaptic *oxIs22* marker in muscles both appear on the ventral side only (top illustration). In *sad-1* mutants, ectopic *juls1* and *oxIs22* signals appear on the dorsal side (bottom illustration). Ectopic dorsal signals (arrowheads) were also apparent in *par-4*(*it57ts*) and *strd-1*(*rr91*) mutants, but the *par-4* polarity phenotype was milder. (**B**) Penetrance of the DD polarity defect. The bars represent the proportion of animals displaying the ectopic dorsal *juls1* (grey) and *oxIs22* (brown) puncta. All counts were different from WT, $P<1\times10^{-11}$, Proportion test; $n>80$ per strain. (**C**) Polarity defects in ventral cord (VD) neurons that innervate ventral body wall muscles in adults. In *wt* animals, VD-derived pre-synaptic *juls1* puncta are excluded from the dorsal side (top illustration) and visualized by *unc-30* RNAi. *sad-1* mutants display ectopic dorsal *juls1* puncta (bottom illustration). Ectopic dorsal puncta were also observed in *par-4*(*it57ts*) and *strd-1*(*rr91*) mutants. (**D**) Quantification of the VD polarity defect. The average number of ectopic dorsal puncta per animal is shown. Values are means ± s.d., $P<1\times10^{-5}$ against WT, Wilcoxon rank-sum test, $n\geq13$ per strain. (**E**) Synaptic organization defect in adult DD neurons. In *wt* adults, DD neuron-derived *juls1* puncta appear round and discrete (left illustration), whereas in *sad-1* mutants, they are diffuse or smaller (right illustration). Representative DD-derived *juls1* morphology in wild-type (i,iii), *par-4*(*it57ts*) (ii), *sad-1* (iv), *strd-1*(*ok2283*) (v) and *strd-1;sad-1* (vi) animals is shown. The distribution of the *juls1* punctum widths from each genotype is plotted in a Kernel density graph. There was no significant difference between wild-type animals and *par-4* mutants ($P>0.05$, *t*-test, $n>90$ per strain), but the distribution curves for *sad-1*, *strd-1* and *sad-1;strd-1* double mutants showed widening patterns, or lower kurtoses, compared with wild-type animals. The distribution curves of *sad-1* and *strd-1* single mutants showed no significant difference compared with *strd-1;sad-1* double mutants ($P>0.05$, *t*-test, $n>60$ per strain). *x*-axis, punctum width in pixels; *y*-axis, arbitrary density unit. Green lines in the illustrations depict the nerve cords; black lines, axonal and dendritic VD (C) or DD (E) projections. Scale bars: 5 μm.

permissive temperatures might not necessarily inactivate all functions of PAR-4, and the mutations in *it33* and *it75* are not completely null. In both *ts* and non-conditional alleles of *par-4* mutants, the maternal contribution of PAR-4 activity might also mask the severity of their polarity defects.

To directly test whether *par-4* and *strd-1* function in the same genetic pathway as *sad-1*, we assessed the phenotypes of *par-4;sad-1*(*null*) and *strd-1;sad-1*(*null*) double loss-of-function mutants. We reasoned that if PAR-4 functions solely through SAD-1, the partial loss-of-function of *par-4* should cause no further enhancement of the polarity defects in the *sad-1*-null background. However, for both *it57ts* and *it33* alleles of *par-4*, the polarity defects in *par-4;sad-1* double mutants were more severe than the respective single mutants in VD neurons (Fig. 2A; also see Fig. S2A in the supplementary material). Such an additive effect was also observed in the ASI neuron for *it57ts;sad-1* (see Fig. S3C in the supplementary material), suggesting that the polarity phenotypes observed in *par-4* mutants were independent of *sad-1*. We could not test *par-4* in the *strd-1* mutant background because *par-4*(*it57ts*)*;strd-1*(*rr91*) and *par-4*(*it33*)*;strd-1(ok2283*) double mutants were embryonically lethal under all conditions.

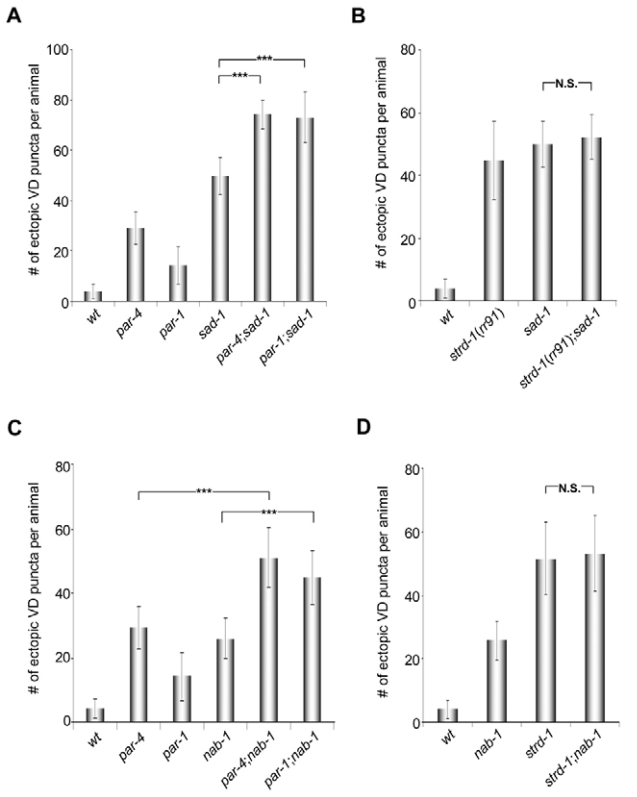

Fig. 2. *sad-1* and *strd-1* function in a pathway parallel to *par-4* and *par-1*. VD polarity phenotypes in adults. (**A**) Defects in *par-4;sad-1* and *par-1;sad-1* mutants. *par-4*(*it57ts*)*;sad-1* and *par-1*(*zu310ts*)*;sad-1* double mutants showed a significant increase in the number of ectopic SNB-1::GFP puncta compared with the respective single mutants. (**B**) Defects in *strd-1;sad-1* double mutants. *strd-1*(*rr91*)*;sad-1* double mutants showed no significant increase in the number of ectopic SNB-1::GFP puncta over their respective single mutants. (**C**,**D**) Defects in *par-4/par-1;nab-1* and *strd-1;nab-1* mutants. Although both *par-4*(*it57ts*) and *par-1*(*zu310ts*) enhanced the polarity defects in *nab-1*(*ok943*) mutants (C), *strd-1*(*ok2283*) did not (D). ***, $P<0.001$; N.S., not significant, Wilcoxon rank-sum test. All values are means ± s.d. $n \geq 10$ per strain.

To further verify these findings, we examined *par-1* mutants. PAR-1, an AMPK-related Ser/Thr kinase, shares the same genetic pathway with PAR-4 to regulate early embryonic cell divisions in *C. elegans* (Watts et al., 2000). *par-1*(*zu310ts*) mutants indeed displayed neuronal polarity defects (Fig. 2A; also see Fig. S3C in the supplementary material) and, similar to *par-4*, *par-1* mutation also enhanced the VD (Fig. 2A) and ASI (see Fig. S3C in the supplementary material) polarity defects in the *sad-1*-null background. Furthermore, the VD polarity defect in *par-1* mutants could be partially rescued by over-expressing PAR-4 in GABAergic neurons (see Fig. S4A in the supplementary material), and the level of VD polarity defect in *par-1;par-4* double mutants showed no enhancement over the single mutants (data not shown), further supporting a shared pathway between the two *par* genes in regulating neuronal polarity.

By contrast, despite having more severe polarity defects than *par-4* and *par-1*, *strd-1* mutants showed no enhancement of the polarity defects in the VD or ASI neurons over the *sad-1*-null background (Fig. 2B; also see Fig. S3D in the supplementary material). These findings suggest that *strd-1* and *sad-1* act in the same genetic pathway. Over-expressing SAD-1 in the *strd-1*(*rr91*) mutant background also partially rescued the VD polarity defect but not vice versa (see Fig. S4B in the supplementary material), consistent with STRD-1 being a pseudokinase that functions through a kinase. Furthermore, no enhancement was observed in the synaptic morphology defect of *strd-1;sad-1* double mutants when compared with the single mutants (Fig. 1E, bottom density graph), indicating that *strd-1* and *sad-1* function together to regulate synaptic organization as well as neuronal polarity.

The co-existence of the separate PAR-1/PAR-4 and STRD-1/SAD-1 functional pathways is supported by all additional genetic interactions we have tested to date. For example, a scaffolding protein Neurabin (NAB-1) functions in the same genetic pathway as SAD-1 to regulate neuronal polarity (Hung et al., 2007). Similar to their genetic interactions with *sad-1* mutants, both *par-4* and *par-1* mutants enhanced the polarity defects of *nab-1* mutants (Fig. 2C), whereas *strd-1*(*ok2283*) mutants, like *sad-1*, did not (Fig. 2D). We also examined RPM-1, an E3 ubiquitin ligase required for pre-synaptic development (Liao et al., 2004; Zhen et al., 2000). Mutations in *rpm-1* lead to severely reduced and uncoordinated locomotion in the *sad-1*-null background (our published observation; see Movies in the supplementary material). Similarly, *strd-1(ok2283);rpm-1* double mutants were also severely lethargic and uncoordinated, whereas both *par-4*(*it57ts*)*;rpm-1* and *par-1;rpm-1* mutants displayed close to normal locomotion similar to their respective single mutants (see Movies in the supplementary material).

These findings and further genetic analyses (see Fig. S4C,D in the supplementary material) indicate that *strd-1* functions in the same genetic pathway as *sad-1* to regulate neuronal polarity and synaptic organization. Although the embryonic lethality of *par-4*-null alleles prevented us from revealing the full role of PAR-4, the polarity defects we were able to observe were genetically independent of *sad-1*, suggesting that PAR-4 is likely to also function through other effectors such as PAR-1. We focused on characterizing the interaction between STRD-1 and SAD-1 henceforth.

STRD-1 is a pseudokinase that functions cell-autonomously in neurons

To investigate the mechanism through which STRD-1 regulates neuronal polarity and synaptic organization, we first analyzed the expression patterns of STRD-1. A transcriptional reporter was

generated by driving GFP expression under the promoter of the operon in which *strd-1* resides. In somatic tissues, GFP reporter signals were detected in the pharynx, excretory canal and entire nervous system (Fig. 3A). The expression pattern of STRD-1 overlaps with that of SAD-1, which is specifically expressed in the nervous system (Crump et al., 2001). We further asked whether STRD-1 functions cell-autonomously in neurons. Expressing STRD-1 exclusively in GABAergic motoneurons using the *unc-25* promoter fully rescued the VD polarity and the DD synaptic organization defects in *strd-1* mutants (Fig. 3B,Ci,ii, density graph). Therefore STRD-1, like SAD-1 (Crump et al., 2001; Hung et al., 2007), functions cell-autonomously in neurons to regulate both neuronal polarity and synaptic organization.

Like mammalian STRADα, STRD-1 lacks some of the essential residues for kinase activity (see Fig. S1 in the supplementary material). These include the DFG motif that is mutated to GFR and the missing threonine and serine residues in the activation loop. The aspartic acid in the catalytic loop for proton transfer that is mutated in STRADα, however, remains intact in STRD-1 (see Fig. S1 in the supplementary material). It raised a possibility that *C. elegans* STRD-1 might be a functional kinase. To test this, we mutated this aspartic acid to alanine (D175A), and STRD-1(D175A) was expressed in GABAergic motoneurons in *strd-1* mutants. Complete rescue of the VD polarity and DD synaptic organization phenotypes was observed (Fig. 3B,Ciii, density curve), suggesting that like its mammalian counterpart, STRD-1 functions as a pseudokinase in *C. elegans*.

STRD-1 co-localizes and forms a complex with SAD-1

To determine the sub-cellular localization of STRD-1, we expressed fluorescently tagged, functional STRD-1 in GABAergic motoneurons. GFP::STRD-1 localized to the soma and the nucleus (Fig. 3D, top panel) and along the neurites in a punctate pattern (Fig. 3D, bottom panel), similar to many synaptic proteins including SAD-1 (Crump et al., 2001). The *sad-1* gene encodes two isoforms with distinct functional specificity (Hung et al., 2007). Whereas the large isoform, SAD-1(L), is sufficient for regulating both neuronal polarity and synaptic organization, the smaller isoform, SAD-1(S), affects only synaptic organization. Both are co-expressed from the *hpIs1* marker [P_{unc-25}-*sad-1*::*gfp*(L,S)]. RFP::STRD-1 extensively co-localized with GFP::SAD-1 puncta when expressed in GABAergic neurons (Fig. 4A). Extensive co-localization was also observed between RFP::STRD-1 and a SAD-1(L) marker *hpIs99* [P_{unc-25}-*gfp*::*sad-1*(L)] (Fig. 4B), as well as the SAD-1(S) marker *hpIs105* [P_{unc-25}-*rfp*::*sad-1*(S)] (Fig. 4C). Therefore STRD-1 is present at synapses and co-localizes with SAD-1.

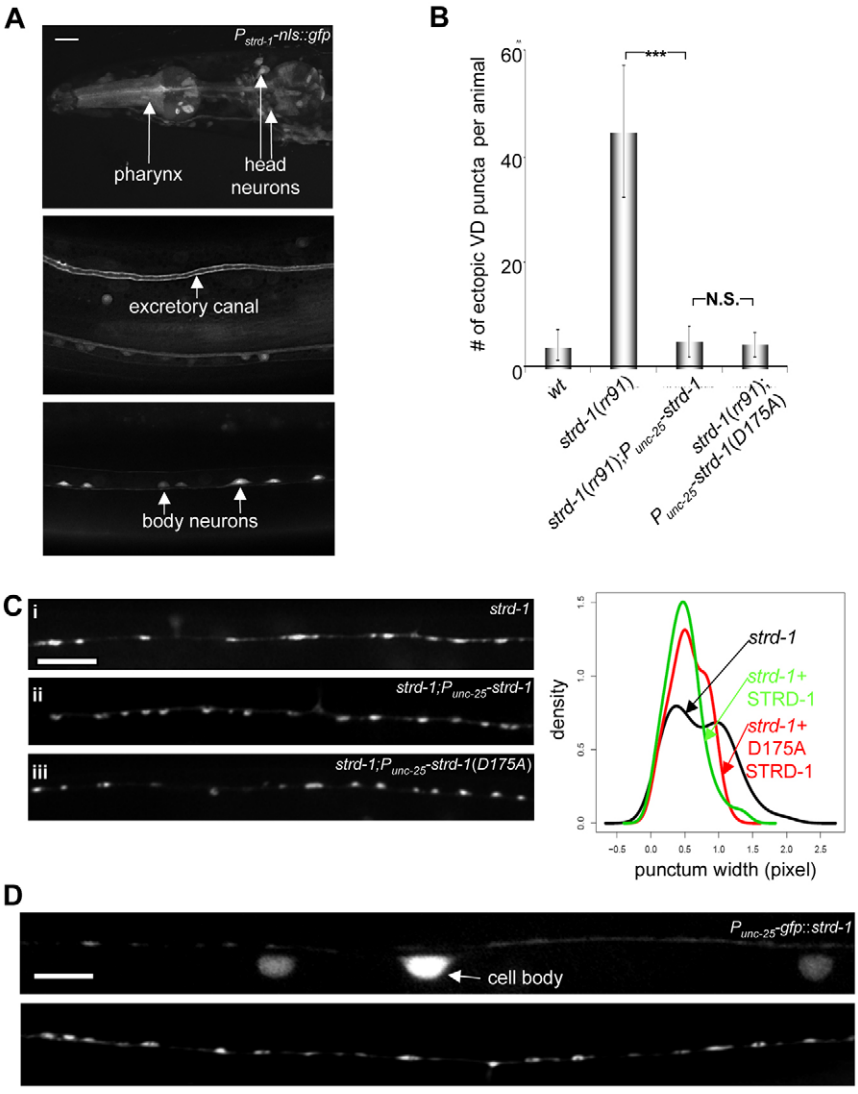

Fig. 3. Pseudokinase STRD-1 functions cell-autonomously in neurons. (**A**) The expression of a P_{strd-1}-*nls*::*gfp* reporter in the pharynx, excretory canal and the entire nervous system. (**B**) Cell-autonomous rescue of the neuronal polarity defect in *strd-1* mutants. The VD polarity defect in *strd-1*(*rr91*) mutant animals was fully rescued by the expression of STRD-1 solely in GABAergic neurons under P_{unc-25}. STRD-1(D175A) also fully rescued the VD polarity defect. Values are means ± s.d.; ***, P<0.001; N.S., not significant, Wilcoxon rank-sum test; n≥10 per strain. (**C**) Cell-autonomous rescue of *strd-1* synaptic organization defect. *strd-1*(*ok2283*) mutants (i) expressing STRD-1 (ii) or STRD-1(D175A) (iii) in GABAergic neurons showed rescued *juIs1* morphology. Distribution of the *juIs1* punctum widths showed significantly reduced kurtoses in the rescued animals (P<0.001, *strd-1* versus either STRD-1-expressing lines, *t*-test; n>80 per strain). *x*-axis, punctum width in pixels; *y*-axis, density in arbitrary units. (**D**) Sub-cellular localization of GFP-tagged, functional STRD-1 in GABAergic neurons. GFP::STRD-1 localized to the cytoplasm and the nucleus as well as along both nerve cords. Scale bars: 5 μm.

The extensive co-localization between STRD-1 and SAD-1, in addition to our genetics data, prompted us to examine whether the two proteins interact in vivo. We first addressed this question by immunoprecipitation. From the lysate of *hpIs99* [$P_{unc\text{-}25}$-*gfp*::*sad-1*(L)] animals, we immunoprecipitated GFP::SAD-1 with anti-GFP and probed it with anti-STRD-1 (Fig. 4D). Endogenous STRD-1 co-immunoprecipitated specifically with GFP::SAD-1(L) from the *hpIs99* lysate, but not from the lysate of *strd-1*(*ok2283*);*hpIs99* or wild-type animals (Fig. 4D), nor from the IgG pull down of the *hpIs99* lysate (data not shown). We further examined whether STRD-1 and SAD-1 associate with each other in vivo via bifluorescent reconstitution, where two split fragments of YFP reconstitute and fluoresce when brought in close proximity by proteins they are fused to (Zhang et al., 2004). The two YFP fragments were tagged to the N-terminus of STRD-1 or SAD-1, respectively, and expressed in GABAergic neurons. YFP fluorescence was detected in animals expressing both fusion proteins (Fig. 4Ei), but not in those expressing either fusion protein with the complementary split YFP vector (Fig. 4Eii,iii), suggesting that STRD-1 and SAD-1 tightly associate with each other in a protein complex in vivo.

STRD-1 affects SAD-1 synaptic localization

Mammalian STRADα affects the cytoplasmic-nuclear translocation, stability and optimal kinase activity of LKB1 in cell cultures. We investigated whether STRD-1 plays similar roles on SAD-1 in vivo. Both GFP- or RFP-tagged SAD-1 isoforms were absent from the nucleus in wild-type animals and *strd-1*(*ok2283*) mutants (Fig. 5A; data not shown). Nuclear exclusion of endogenous SAD-1 was also observed in wild-type animals and *strd-1* mutants (Fig. 5D, middle panels, arrowheads). Therefore, STRD-1 is unlikely to shuttle SAD-1 from the nucleus to the cytoplasm in mature neurons.

Because both STRD-1 and SAD-1 localized to synaptic regions (Fig. 4A-C), we examined whether STRD-1 affects the localization of SAD-1 at synapses. Compared with wild-type animals, in *strd-1*(*ok2283*) mutants fewer puncta and more diffuse fluorescence along the dorsal nerve cord were observed with the *hpIs1* marker (Fig. 5Bi-ii,C), indicating that SAD-1::GFP(L,S) was mislocalized in *strd-1* mutants. Interestingly, when further examined with isoform-specific SAD-1 markers, the synaptic localization of the long isoform was preferentially affected in *strd-1* mutants (Fig. 5Biii-iv versus Cv-vi). A reciprocal examination of the sub-cellular localization of GFP::STRD-1 in *sad-1* mutants did not reveal drastic changes (data not shown), suggesting that GFP::STRD-1 localization was largely independent of SAD-1. We did not observe obvious changes of SAD-1::GFP or GFP::STRD-1 localization in *par-4(it33)* (not shown), suggesting that their subcellular localizations do not critically depend on PAR-4 activity.

We also examined the level and localization of endogenous SAD-1 in wild-type animals and *strd-1*(*ok2283*) mutants by antibody staining for SAD-1. There was no gross change in the level of SAD-

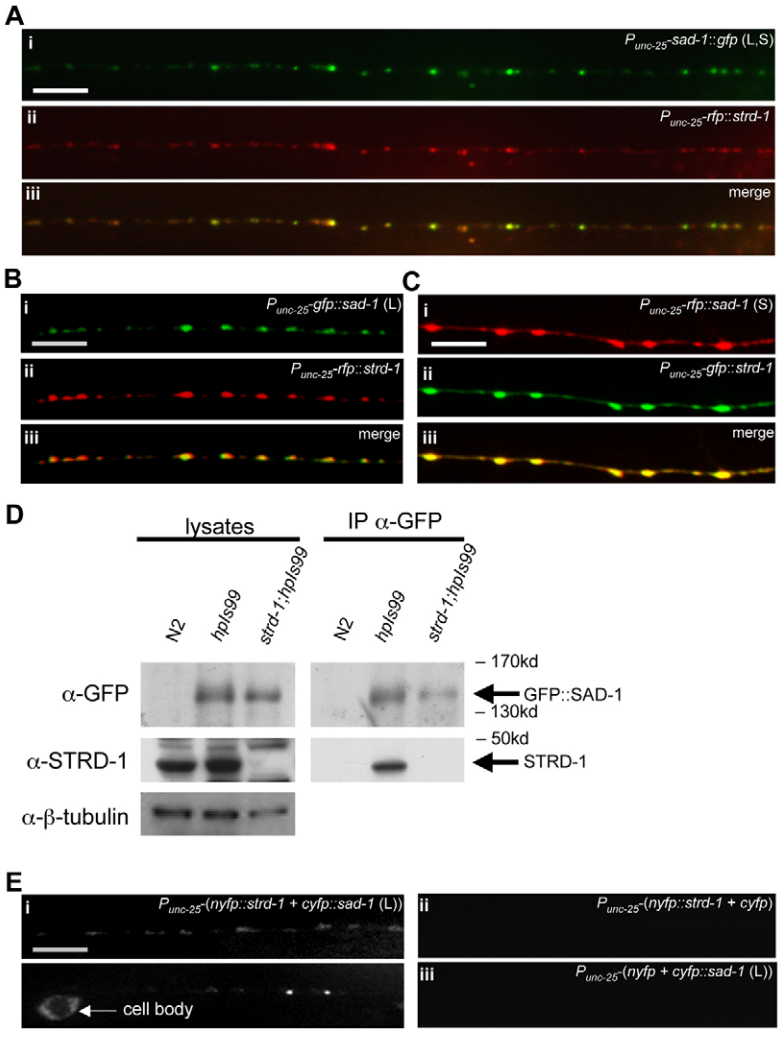

Fig. 4. STRD-1 and SAD-1 co-localize and interact in vivo. (**A-C**) Sub-cellular co-localization of STRD-1 with SAD-1 along the dorsal nerve cord. Expressed in GABAergic neurons, RFP- (A,B) or GFP- (C) tagged STRD-1 extensively co-localized with *hpIs1* (expressing both isoforms of SAD-1 tagged to GFP) (A), *hpIs99* [expressing GFP::SAD-1(L)] (B), and *hpIs105* [expressing RFP::SAD-1(S)] (C). (**D**) Co-immunoprecipitation of endogenous STRD-1 with GFP::SAD-1(L) in *C. elegans*. Lysates from *hpIs99*, *strd-1*(*ok2283*);*hpIs99* and wild-type animals were immunoprecipitated with anti-GFP and probed with anti-STRD-1. STRD-1 specifically co-immunoprecipitated with GFP::SAD-1(L). There was no significant change in the gross level of GFP::SAD-1 in *strd-1* mutants. (**E**) Associations between STRD-1 and SAD-1 in vivo. N- or C-terminus fragments of YFP were tagged to STRD-1 and SAD-1(L), respectively, and expressed in GABAergic neurons. YFP fluorescence was observed in animals expressing both proteins (i) along the dorsal (top panel) and ventral (bottom panel) nerve cords, but not in those expressing one fusion protein with the tag vector for the counter construct (ii,iii). Scale bars: 5 μm.

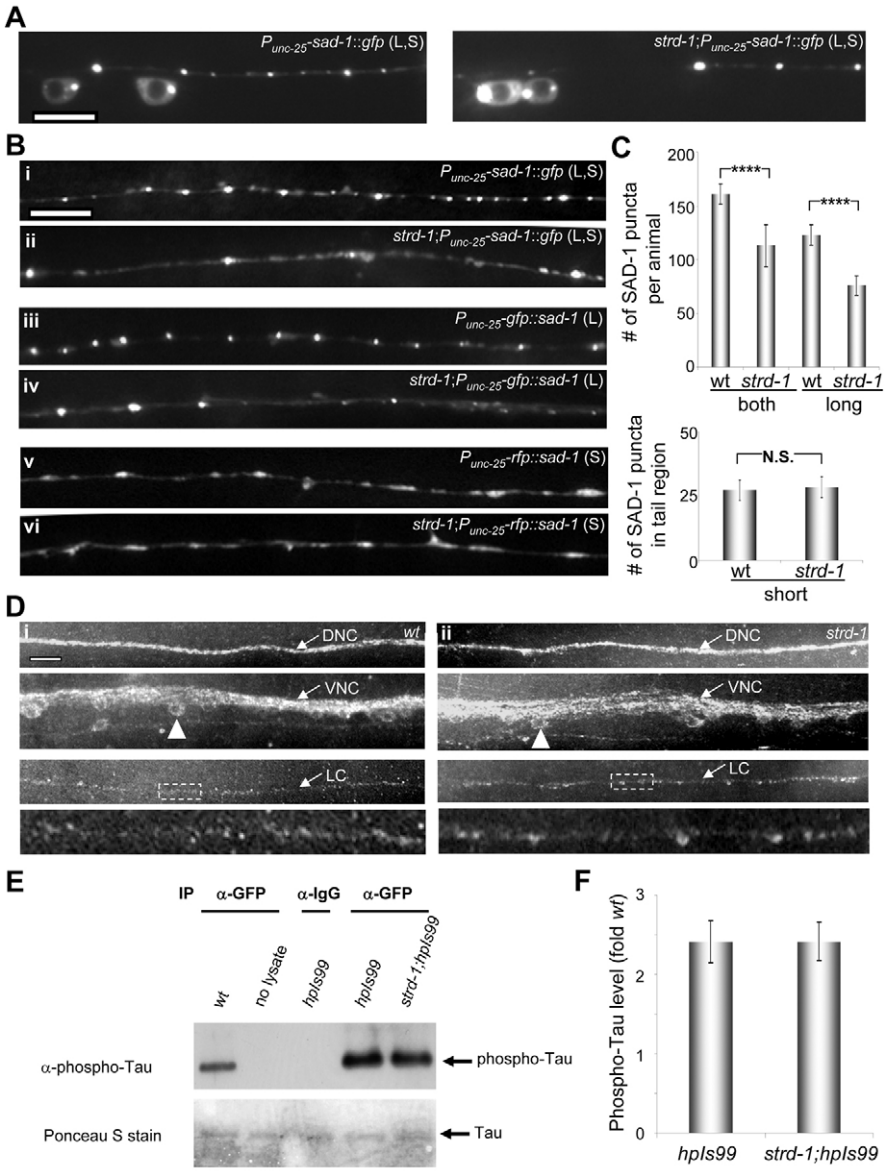

Fig. 5. STRD-1 modulates synaptic localization of SAD-1. (**A**) Sub-cellular localization of SAD-1 in the cell bodies of wild-type animals and *strd-1* mutants. SAD-1::GFP(L,S) in *hpIs1* animals is excluded from the nucleus in both wild-type and *strd-1*(*ok2283*) animals. (**B**) Sub-cellular localization of SAD-1 along the dorsal nerve cord in wild-type and *strd-1* mutant animals. In *strd-1*(*ok2283*) mutants, some bright GFP signals from the *hpIs1* [GFP::SAD-1(L,S)] (i,ii) and from the *hpIs99* [GFP::SAD-1(L)] (iii,iv) animals became diffuse and sporadic. No obvious difference was observed with the marker expressing the more diffuse RFP::SAD-1(S) only (v,vi). (**C**) Quantification of the number of bright GFP puncta between wild-type and *strd-1* animals. The number of GFP puncta in *strd-1* mutants was reduced for both lines expressing SAD-1(L) but not for SAD-1(S). Values are means ± s.d.; ****, $P<0.0001$, N.S., not significant, *t*-test. $n\geq10$ per strain. (**D**) Endogenous SAD-1 staining patterns in wild-type (i) and *strd-1* (ii) animals. No obvious change was detected along the bundled nerve cords or in the cell body (arrowheads) between wild-type (*wt*) animals and *strd-1*(*ok2283*) mutants (top panels). Along ventral lateral cords (LC), SAD-1 was more diffuse and unevenly localized in *strd-1* mutants (ii, bottom two panels) when compared with wild-type animals (i, bottom two panels). (**E**,**F**) In vitro SAD-1 kinase activity in the presence and absence of STRD-1. GFP::SAD-1 complex that was immunoprecipitated from wild-type animals and *strd-1*(*ok2283*) mutants, as in Fig. 4D, displayed similar basal level activities in phosphorylating Tau in vitro. $n=3$ for F. Scale bars: 5 μm.

1 staining (Fig. 5D), suggesting that STRD-1 has little effect on the stability of SAD-1. This finding is consistent with the comparable level of GFP::SAD-1 between wild-type animals and *strd-1*(*ok2283*) mutants (Fig. 4D). The dorsal and ventral nerve cords also appeared similar between wild-type animals and *strd-1* mutants (Fig. 5D, top two panels). However, as both regions have densely overlaid synapses that may mask subtle localization changes, we examined SAD-1 staining at regions of single synapse resolution. Lateral cords comprise only single or a few axons, allowing the visualization of single synapses. Although SAD-1 staining appeared discretely punctate and evenly spaced along the lateral cords in wild-type animals (Fig. 5Di, bottom two panels), more diffuse staining with gaps was observed in *strd-1* mutants (Fig. 5Dii, bottom two panels). Therefore, both marker expression and endogenous staining experiments suggest that STRD-1 is required for the punctate SAD-1 localization at synapses.

To address whether STRD-1 also affects the kinase activity of SAD-1, GFP::SAD-1 that was immunoprecipitated from *hpIs99* and *strd-1*(*ok2283*);*hpIs99* animals (as in Fig. 4D) was subjected to an in vitro kinase assay with the sole known substrate of mammalian SADs, Tau. GFP::SAD-1 from wild-type animals and *strd-1* mutants displayed similar kinase activities in phosphorylating Tau (Fig. 5E-F), suggesting that the activity of SAD-1 is not affected by STRD-1 in vitro. This finding, however, does not exclude the possibility that, in vivo, STRD-1 is required for SAD-1 kinase activity on its endogenous substrate(s) upon activation.

DISCUSSION

The SAD kinases are essential for specifying axon-dendrite identity in developing neurons (Barnes et al., 2007; Kim et al., 2008; Kishi et al., 2005). Recent studies suggest that LKB1 regulates the polarity of developing mouse cortical neurons through activating the SAD kinases (Barnes et al., 2007). Consistent with these findings, PAR-4 also functions cell-autonomously in regulating neuronal polarity in *C. elegans* (see Fig. S4A in the supplementary material). Although the endogenous expression patterns of post-embryonic PAR-4 are unknown, we observed its neuronal expression using a transcriptional reporter (data not shown). Our temperature-shift experiments further indicated that PAR-4 activity is crucial during the establishment of neuronal polarity (see Fig. S2B in the supplementary material).

STRADα was implicated in LKB1-mediated neuronal polarization (Barnes et al., 2007; Shelly et al., 2007), but the analysis of STRADα loss-of-function mutants has yet to be described. Lacking some of the essential residues for kinase activity, *C. elegans* STRD-1, like STRADα, functions through other kinases. We found that *strd-1* loss-of-function mutants phenocopied the neuronal defects of *sad-1* mutants, and *strd-1;sad-1* double mutants mimicked the single mutants. *strd-1* mutants also displayed slightly shallower and more stiff sinusoidal waves in locomotion, a subtle behavioural deficit that was identical to and characteristic of *sad-1* mutants (see Movies in the supplementary material). By contrast, *par-4* mutants not only exhibit milder polarity defects when compared with *sad-1* and *strd-1* mutants, but these defects also appeared additive in *par-4;sad-1* mutants. Our findings establish STRD-1 as a key regulator of neuronal polarity and synaptic organization functioning through the SAD-1 kinase in vivo.

STRADα is a component of the LKB1/STRAD/MO25 trimeric complex that affects the stability, localization and optimal activity of LKB1 in various cell culture studies (Baas et al., 2003; Boudeau et al., 2003; Lizcano et al., 2004). It was therefore unexpected to identify consistent differences in the phenotypic severity between *par-4* and *strd-1* mutants, and, moreover, between their genetic interactions with *sad-1*. The simplest explanation for the milder phenotypes of *par-4* mutants is that the residual PAR-4 activity is sufficient to activate SAD-1 in the presence of STRD-1. Nevertheless, the enhancements in the polarity defects of *par-4;sad-1* double mutants unambiguously revealed an additional, *sad-1*-independent genetic pathway through which *par-4* regulates neuronal polarity.

This SAD-1/STRD-1-independent PAR-4 function is likely to be through the conserved PAR-4/PAR-1 kinase cascade that regulates the polarity of non-neuronal tissues (Amin et al., 2009; Kemphues et al., 1988; Martin and St Johnston, 2003). Apart from the evidence presented above, the co-existence of the PAR-1/PAR-4 and STRD-1/SAD-1 functional pathways is supported by additional genetic interactions. For example, consistent with previous studies that placed mammalian and *Drosophila* PAR proteins downstream of the *wnt* signalling (Spicer et al., 2003; Sun et al., 2001), mutations in *dsh-2*, a *C. elegans Disheveled* gene, did not enhance the VD polarity defects of either *par-4* or *par-1* mutants (see Fig. S4C in the supplementary material). By contrast, *dsh-2* significantly enhanced the defects of both *strd-1* and *sad-1* mutants (see Fig. S4D in the supplementary material). A completely normal localization of GFP::SAD-1(L) in *par-4* mutants (see Fig. S5 in the supplementary material) is also consistent with the presence of additional effectors of PAR-4 in neuronal polarity.

Future studies are needed to identify additional activators or regulators of SAD-1. We have not determined whether *C. elegans* homologues for MO25, MOP-25.1, MOP-25.2 and a more divergent MOP-25.3, participate in SAD-1-mediated neuronal development. Aside from LKB1, other candidate SAD activators include a Ca^{2+}/calmodulin-dependent protein kinase, recently shown to be a potent activator for SAD-B in vitro (Fujimoto et al., 2008), and the Tuberous Sclerosis Complex Tsc1-Tsc2, also found to modulate the activity of SAD kinases in cultured neurons (Choi et al., 2008). Regardless of which kinase(s) activate SAD-1, the identical neuronal phenotypes among *strd-1*, *sad-1* and *strd-1*;*sad-1* mutants predict that STRD-1 is involved in this process. Although STRD-1 does not affect SAD-1-mediated Tau-phosphorylation in vitro, it does not dismiss the possibility that STRD-1 is required for SAD-1 activation and/or the phosphorylation of its endogenous substrates in vivo.

We demonstrated by both immunoprecipitation and YFP bifluorescent reconstitution that STRD-1 forms a stable protein complex with SAD-1. This is intriguing, as STRADα has only been previously described in the context of the LKB1 complex. About fifty pseudokinases have been identified in the human genome (Boudeau et al., 2006). Together with our findings, this implies that the formation of complexes between a pseudokinase and a kinase could prove to be more prevalent and promiscuous for many other kinases.

STRD-1 also has functions distinct from SAD-1. It is expressed in several tissues besides the nervous system, to which SAD-1 expression is restricted. Indeed, *strd-1* mutants display germline defects similar to *par-4* mutants, whereas *sad-1* mutants do not (P.N. and R.R., unpublished). This observation supports our premise that STRD-1 is a promiscuous pseudokinase capable of functioning through multiple binding partners in different cellular contexts (e.g. early embryogenesis versus neural differentiation). Interestingly, human genetic studies have noted that unlike LKB1, mutations in STRADα are not associated with the cancer-developing Peutz-Jeghers syndrome (Alhopuro et al., 2005; de Leng et al., 2005); instead, a deletion in STRADα leads to distinct clinical features including abnormal brain and craniofacial development (Puffenberger et al., 2007). This might also provide an alternative explanation for the observation in dissociated mouse cortical neurons where the supernumerary axon phenotype induced by LKB1/STRADα co-expression was only partially blocked by siRNA-mediated knock-down of SAD-A and SAD-B (Barnes and Polleux, 2009).

In summary, instead of having only dedicated functions through LKB1, *C. elegans* STRADα/STRD-1 forms a complex with and functions through the SAD-1 kinase to regulate neuronal polarity and synaptic organization. Moreover, the first direct genetic analyses between the *C. elegans* STRADα, LKB1 and SAD mutants revealed separate genetic pathways through which LKB1 and SAD regulate neuronal polarity. It will be important to examine STRADα knock-out mutants and also other AMPK kinases including PAR-1 as additional effectors of LKB1 in establishing neuronal polarity in vertebrates.

Acknowledgements

We thank K. J. Kemphues for strains, J.-C. Labbé for *par-4* cDNA, Z. W. Wang for split-*yfp* tags, A. Desai for the *wCherry* construct, C. G. C. for strains, T. Kaneko for antibodies against GFP, C. Mok and T. Kawano for Punctaanalyser, P. C. Boutros for assistance in statistical analyses and J. Calarco, B. N. Lilley, H. McNeill and J. R. Sanes for comments on the manuscript. This work was supported by an NSERC fellowship to J.S.M.K., a CIHR grant to R.R. and a CIHR and an NSERC grant to M.Z.

Supplementary material

Supplementary material available online at
http://dev.biologists.org/lookup/suppl/doi:10.1242/dev.041459/-/DC1

References

Alhopuro, P., Katajisto, P., Lehtonen, R., Ylisaukko-Oja, S. K., Naatsaari, L., Karhu, A., Westerman, A. M., Wilson, J. H., de Rooij, F. W., Vogel, T. et al. (2005). Mutation analysis of three genes encoding novel LKB1-interacting proteins, BRG1, STRADalpha, and MO25alpha, in Peutz-Jeghers syndrome. *Br. J. Cancer* **92**, 1126-1129.

Amin, N., Khan, A., St Johnston, D., Tomlinson, I., Martin, S., Brenman, J. and McNeill, H. (2009). LKB1 regulates polarity remodeling and adherens junction formation in the Drosophila eye. *Proc. Natl. Acad. Sci. USA* **106**, 8941-8946.

Arimura, N. and Kaibuchi, K. (2005). Key regulators in neuronal polarity. *Neuron* **48**, 881-884.

Baas, A. F., Boudeau, J., Sapkota, G. P., Smit, L., Medema, R., Morrice, N. A., Alessi, D. R. and Clevers, H. C. (2003). Activation of the tumour suppressor kinase LKB1 by the STE20-like pseudokinase STRAD. *EMBO J.* **22**, 3062-3072.

Baas, A. F., Kuipers, J., van der Wel, N. N., Batlle, E., Koerten, H. K., Peters, P. J. and Clevers, H. C. (2004). Complete polarization of single intestinal epithelial cells upon activation of LKB1 by STRAD. *Cell* **116**, 457-466.
Barnes, A. P. and Polleux, F. (2009). Establishment of axon-dendrite polarity in developing neurons. *Annu. Rev. Neurosci.* **32**, 347-381.
Barnes, A. P., Lilley, B. N., Pan, Y. A., Plummer, L. J., Powell, A. W., Raines, A. N., Sanes, J. R. and Polleux, F. (2007). LKB1 and SAD kinases define a pathway required for the polarization of cortical neurons. *Cell* **129**, 549-563.
Boudeau, J., Baas, A. F., Deak, M., Morrice, N. A., Kieloch, A., Schutkowski, M., Prescott, A. R., Clevers, H. C. and Alessi, D. R. (2003). MO25alpha/beta interact with STRADalpha/beta enhancing their ability to bind, activate and localize LKB1 in the cytoplasm. *EMBO J.* **22**, 5102-5114.
Boudeau, J., Scott, J. W., Resta, N., Deak, M., Kieloch, A., Komander, D., Hardie, D. G., Prescott, A. R., van Aalten, D. M. and Alessi, D. R. (2004). Analysis of the LKB1-STRAD-MO25 complex. *J. Cell Sci.* **117**, 6365-6375.
Boudeau, J., Miranda-Saavedra, D., Barton, G. J. and Alessi, D. R. (2006). Emerging roles of pseudokinases. *Trends Cell Biol.* **16**, 443-452.
Brenner, S. (1974). The genetics of *Caenorhabditis elegans*. *Genetics* **77**, 71-94.
Choi, Y. J., Di Nardo, A., Kramvis, I., Meikle, L., Kwiatkowski, D. J., Sahin, M. and He, X. (2008). Tuberous sclerosis complex proteins control axon formation. *Genes Dev.* **22**, 2485-2495.
Conde, C. and Caceres, A. (2009). Microtubule assembly, organization and dynamics in axons and dendrites. *Nat. Rev. Neurosci.* **10**, 319-332.
Crump, J. G., Zhen, M., Jin, Y. and Bargmann, C. I. (2001). The SAD-1 kinase regulates pre-synaptic vesicle clustering and axon termination. *Neuron* **29**, 115-129.
de Leng, W. W., Keller, J. J., Luiten, S., Musler, A. R., Jansen, M., Baas, A. F., de Rooij, F. W., Gille, J. J., Menko, F. H., Offerhaus, G. J. et al. (2005). STRAD in Peutz-Jeghers syndrome and sporadic cancers. *J. Clin. Pathol.* **58**, 1091-1095.
Dorfman, J. and Macara, I. G. (2008). STRADalpha regulates LKB1 localization by blocking access to importin-alpha, and by association with Crm1 and exportin-7. *Mol. Biol. Cell* **19**, 1614-1626.
Dotti, C. G., Sullivan, C. A. and Banker, G. A. (1988). The establishment of polarity by hippocampal neurons in culture. *J. Neurosci.* **8**, 1454-1468.
Dwyer, N. D., Adler, C. E., Crump, J. G., L'Etoile, N. D. and Bargmann, C. I. (2001). Polarized dendritic transport and the AP-1 mu1 clathrin adaptor UNC-101 localize odorant receptors to olfactory cilia. *Neuron* **31**, 277-287.
Fire, A., Xu, S., Montgomery, M. K., Kostas, S. A., Driver, S. E. and Mello, C. C. (1998). Potent and specific genetic interference by double-stranded RNA in *Caenorhabditis elegans*. *Nature* **391**, 806-811.
Fujimoto, T., Yurimoto, S., Hatano, N., Nozaki, N., Sueyoshi, N., Kameshita, I., Mizutani, A., Mikoshiba, K., Kobayashi, R. and Tokumitsu, H. (2008). Activation of SAD kinase by Ca2+/calmodulin-dependent protein kinase kinase. *Biochemistry* **47**, 4151-4159.
Hallam, S. J., Goncharov, A., McEwen, J., Baran, R. and Jin, Y. (2002). SYD-1, a pre-synaptic protein with PDZ, C2 and rhoGAP-like domains, specifies axon identity in *C. elegans*. *Nat. Neurosci.* **5**, 1137-1146.
Hung, W., Hwang, C., Po, M. D. and Zhen, M. (2007). Neuronal polarity is regulated by a direct interaction between a scaffolding protein, Neurabin, and a pre-synaptic SAD-1 kinase in *Caenorhabditis elegans*. *Development* **134**, 237-249.
Inoue, E., Mochida, S., Takagi, H., Higa, S., Deguchi-Tawarada, M., Takao-Rikitsu, E., Inoue, M., Yao, I., Takeuchi, K., Kitajima, I. et al. (2006). SAD: a pre-synaptic kinase associated with synaptic vesicles and the active zone cytomatrix that regulates neurotransmitter release. *Neuron* **50**, 261-275.
Kemphues, K. J., Priess, J. R., Morton, D. G. and Cheng, N. S. (1988). Identification of genes required for cytoplasmic localization in early *C. elegans* embryos. *Cell* **52**, 311-320.
Kim, J. S., Lilley, B. N., Zhang, C., Shokat, K. M., Sanes, J. R. and Zhen, M. (2008). A chemical-genetic strategy reveals distinct temporal requirements for SAD-1 kinase in neuronal polarization and synapse formation. *Neural Dev.* **3**, 23.
Kishi, M., Pan, Y. A., Crump, J. G. and Sanes, J. R. (2005). Mammalian SAD kinases are required for neuronal polarization. *Science* **307**, 929-932.
Liao, E. H., Hung, W., Abrams, B. and Zhen, M. (2004). An SCF-like ubiquitin ligase complex that controls pre-synaptic differentiation. *Nature* **430**, 345-350.
Lizcano, J. M., Goransson, O., Toth, R., Deak, M., Morrice, N. A., Boudeau, J., Hawley, S. A., Udd, L., Makela, T. P., Hardie, D. G. et al. (2004). LKB1 is a master kinase that activates 13 kinases of the AMPK subfamily, including MARK/PAR-1. *EMBO J.* **23**, 833-843.
Martin, S. G. and St Johnston, D. (2003). A role for Drosophila LKB1 in anterior-posterior axis formation and epithelial polarity. *Nature* **421**, 379-384.
Milburn, C. C., Boudeau, J., Deak, M., Alessi, D. R. and van Aalten, D. M. (2004). Crystal structure of MO25 alpha in complex with the C terminus of the pseudo kinase STE20-related adaptor. *Nat. Struct. Mol. Biol.* **11**, 193-200.
Morton, D. G., Roos, J. M. and Kemphues, K. J. (1992). par-4, a gene required for cytoplasmic localization and determination of specific cell types in *Caenorhabditis elegans* embryogenesis. *Genetics* **130**, 771-790.
Nakamura, K. C., Kameda, H., Koshimizu, Y., Yanagawa, Y. and Kaneko, T. (2008). Production and histological application of affinity-purified antibodies to heat-denatured green fluorescent protein. *J. Histochem. Cytochem.* **56**, 647-657.
Puffenberger, E. G., Strauss, K. A., Ramsey, K. E., Craig, D. W., Stephan, D. A., Robinson, D. L., Hendrickson, C. L., Gottlieb, S., Ramsay, D. A., Siu, V. M. et al. (2007). Polyhydramnios, megalencephaly and symptomatic epilepsy caused by a homozygous 7-kilobase deletion in LYK5. *Brain* **130**, 1929-1941.
Shelly, M., Cancedda, L., Heilshorn, S., Sumbre, G. and Poo, M. M. (2007). LKB1/STRAD promotes axon initiation during neuronal polarization. *Cell* **129**, 565-577.
Spicer, J., Rayter, S., Young, N., Elliott, R., Ashworth, A. and Smith, D. (2003). Regulation of the Wnt signalling component PAR1A by the Peutz-Jeghers syndrome kinase LKB1. *Oncogene* **22**, 4752-4756.
Sun, T. Q., Lu, B., Feng, J. J., Reinhard, C., Jan, Y. N., Fantl, W. J. and Williams, L. T. (2001). PAR-1 is a Dishevelled-associated kinase and a positive regulator of Wnt signalling. *Nat. Cell Biol.* **3**, 628-636.
Watts, J. L., Morton, D. G., Bestman, J. and Kemphues, K. J. (2000). The *C. elegans* par-4 gene encodes a putative serine-threonine kinase required for establishing embryonic asymmetry. *Development* **127**, 1467-1475.
Wiggin, G. R., Fawcett, J. P. and Pawson, T. (2005). Polarity proteins in axon specification and synaptogenesis. *Dev. Cell* **8**, 803-816.
Zhang, S., Ma, C. and Chalfie, M. (2004). Combinatorial marking of cells and organelles with reconstituted fluorescent proteins. *Cell* **119**, 137-144.
Zhen, M. and Jin, Y. (1999). The liprin protein SYD-2 regulates the differentiation of pre-synaptic termini in *C. Elegans*. *Nature* **401**, 371-375.
Zhen, M., Huang, X., Bamber, B. and Jin, Y. (2000). Regulation of pre-synaptic terminal organization by *C. elegans* RPM-1, a putative guanine nucleotide exchanger with a RING-H2 finger domain. *Neuron* **26**, 331-343.